Chinese Journal of
POLYMER SCIENCE

RESEARCH ARTICLE

https://doi.org/10.1007/s10118-026-3778-3
Chinese J. Polym. Sci.

Effect of External Stimuli-triggered Hydrophobic-Hydrophilic Transition on the Disassembly of ABCA Tetrablock Asymmetric Vesicles: a Monte Carlo Simulation Study

Yan-Qi Zong, Jie Cui*, and Yuan-Yuan Han*

School of New Energy and Advanced Materials, Liaoning Petrochemical University, Fushun 113001, China

Abstract Various external stimuli, such as pH, light, and temperature, have been widely used to trigger the hydrophobic-hydrophilic transition of a certain block in block copolymer, which has become a commonly used and effective strategy to induce the disassembly of vesicles for controlled drug release. Based on this, the disassembly behavior of the ABCA tetrablock asymmetric vesicles induced by the hydrophobic-hydrophilic transition of block C was studied using Monte Carlo simulation. In this work, the hydrophobicity of block C was tuned to mimic the hydrophobic-hydrophilic transition triggered by external stimuli. As the hydrophobicity of block C decreases, the initial ABCA asymmetric vesicles disassemble into a series of ordered aggregates such as Janus lamella, reversed asymmetric vesicle, toroid micelle, ring-like micelle and cylindrical micelle. It should be noted that these aggregates disassembled from the initial vesicle state cannot be obtained through the traditional self-assembly method from homogeneous states of the ABCA tetrablock terpolymers under the same conditions. The simulation results show that the hydrophobicity changing rate of block C has a significant effect on the disassembly pathway from the initial asymmetric vesicle to the reversed asymmetric vesicle. It is found that during the disassembly from the initial to the reversed vesicles, the system will undergo an energy-driven process first, then followed by an entropy-driven process. In addition, the simulation results further indicate that the disassembly behavior of the initial ABCA asymmetric vesicles is irreversible.

Keywords Disassembly; Tetrablock terpolymer; Vesicle; Monte Carlo simulation; Selective solvent

Citation: Zong, Y. Q.; Cui, J.; Han, Y. Y. Effect of external stimuli-triggered hydrophobic-hydrophilic transition on the disassembly of ABCA tetrablock asymmetric vesicles: a Monte Carlo simulation study. *Chinese J. Polym. Sci*. https://doi.org/10.1007/s10118-026-3778-3

INTRODUCTION

Amphiphilic block copolymers can spontaneously self-assemble into vesicles with unique aqueous cavities that are enclosed by hydrophobic membranes. This unique structure endows vesicles with great abilities to simultaneously load and deliver hydrophilic drugs within the aqueous cavity and hydrophobic drugs within the membrane, which is conducive to realize synergistic therapeutic effect of drugs. In the past decades, block copolymer vesicles have gained extensive attention in the fields of drug loading and delivery.[1–5] Besides drug loading and delivery, controlled release of the drugs loaded in vesicles is also critical for polymer vesicles in various applications such as disease diagnosis and treatment. In general, drugs can be released from vesicles in a controlled manner through various stimuli such as pH,[6,7] light,[8,9] temperature,[10] and so on. Under the influence of stimuli, the membrane structures of vesicles are usually altered or even destroyed by the stimuli, which results in the disassembly of the vesicles.

* Corresponding authors, E-mail: cuijie@lnpu.edu.cn (J.C.)
E-mail: hanyuanyuan@lnpu.edu.cn (Y.Y.H.)
Received May 7, 2026; Accepted June 9, 2026; Published online August 19, 2026

The disassembly of vesicles triggered by various stimuli has great effects on the controllable drug release of vesicles, hence significantly affecting the therapeutic efficacy. Great attention has long been attracted on the disassembly of vesicles triggered by the stimuli. Among various mechanisms for vesicle disassembly, the stimuli-triggered hydrophobic- hydrophilic transition of the membrane-forming blocks of vesicles plays a very important role in the disassembly of vesicles. For instance, Poly(4-vinylpyridine) (P4VP) is a pH-sensitive block that is commonly used in experiments. When pH<4, the P4VP block is hydrophilic due to the full protonation of the pyridine group under acidic environment, while under alkaline condition (*i.e.*, pH>7), the P4VP block becomes hydrophobic because of the deprotonation of the pyridine group. Based on the pH-triggered hydrophobic- hydrophilic transition of the membrane-forming P4VP block, controllable morphology and structural transition of various ordered aggregates has been successfully achieved by many researchers.[11–13] Besides P4VP, Xu *et al*.[6] fabricated a series of vesicles with different contents of pH-sensitive 2-(diisopropylamino) ethyl methacrylate (DIPEMA) in the vesicle membranes. By decreasing the pH value from neutral condition to pH=4.0, the membrane-forming blocks can be tuned

from hydrophobic to hydrophilic, resulting in the disassembly of the vesicles either quickly into homogeneous unimers, or slowly into small irregular nanoparticles. This behavior can be used to tune the release rate of hydrophilic payloads, such as Rhodamine B. The pH-sensitive DIPEMA was also used by Chen *et al*.[14] to regulate the membrane permeability of vesicles and by Lomas *et al*.[15] to encapsulate and deliver DNA molecules. Moreover, Ge's group[16,17] achieved pH-tunable selective membrane permeability for stimuli-responsive smart drug delivery and controllable enzymatic reaction by incorporating 2-(piperidin-1-yl)ethyl methacrylate (PEMA) into the membrane-forming blocks. PEMA endows the vesicle membrane with pH-responsiveness, *i.e.*, the neutrally hydrophobic vesicle membrane at pH=7.4 will transform into positively hydrophilic one at pH=6.5, and if the membrane was not cross-linked, the vesicles will immediately disassemble into small micellar nanoparticles. In addition to pH sensitive blocks, temperature-induced disassembly of vesicles has attracted increasing attentions of researchers in recent years due to the better controllability of temperature. Temperature-sensitive blocks, such as poly(*N*-isopropylacrylamide) (PNIPAM),[18,19] poly(propylene oxide) (PPO),[20] and poly(*N*-vinylcaprolactam) (PVCL),[21] have been used in drug delivery and controlled release of vesicles. Taking PNIPAM as an example, when the temperature is above the lower critical solution temperature (LCST, about 32 °C), PNIPAM is hydrophobic and collapses in water. As the temperature is decreased lower than the LCST, PNIPAM exhibits hydrophilic property and extends in water.[22] Utilizing this temperature-dependence of hydrophobic-hydrophilic transition of PNIPAM, He *et al*. achieved the switch of the permeability of vesicular membrane toward small molecular substrates between "on" and "off".[18] Besides temperature, light is another convenient and non-contact tuning method that is commonly used in experiments. Light-sensitive moieties such as azobenzene and spiropyran usually have unique light-isomerization features.[23,24] For example, the configuration of azobenzene can be reversibly transformed between *trans*- and *cis*- under the alternating exposure to UV and visible light, which results in a reversible transition of azobenzene between hydrophobic and hydrophilic states. Accordingly, the hydrophobic- hydrophilic properties of the azobenzene-decorated membrane-forming blocks can be reversibly regulated. By introducing light-sensitive moieties, people have realized light-triggered disassembly of vesicles to achieve reversible vesicle-to-worm transition,[25,26] as well as controlled precise release of various drugs.[26–28]

The above experimental investigations indicate that the external stimuli-triggered hydrophobic-hydrophilic (or *vice versa*) transition of the membrane-forming block in an amphiphilic block copolymer has profound effects on the disassembly behavior of vesicles. To further reveal the disassembly behavior of polymer vesicles, computer simulations have also been employed to investigate the effects of vesicle disassembly on drug release since they can reveal microscopic processes at the molecular scale that cannot be discerned directly by experiments only, which is beneficial for deep understanding of the mechanisms for controlled drug loading and release of vesicles.[2,29–33] In computer simulations, the hydrophobic-hydrophilic (or *vice versa*) transition of the membrane-forming blocks or drug molecules can be easily achieved by tuning interaction parameters between corresponding blocks (or drug molecules) with solvents, which provides great convenience for deep study of external-stimuli triggered disassembly and drug release behavior of block copolymer vesicles through computer simulations. Using dissipative particle dynamics (DPD) simulations, Wang's group studied the effects of external stimuli-triggered hydrophobic-hydrophilic transition of drugs and membrane-forming blocks on the kinetics of drug release from vesicles.[4,34] Luo *et al*. has carried out multiscale simulation studies to investigate the loading and release of anti-cancer drugs as well as the disassembly of pH-sensitive vesicles by synergizing molecular dynamics and DPD simulations.[35,36] In addition, Ma *et al*. once studied the spontaneous vesicle formation of ABABA type amphiphilic multiblock copolymers bearing thermosensitive hydrophilic A-block in a selective solvent by DPD simulations.[37]

Up to now, almost all the experimental and simulation studies about the disassembly of amphiphilic block copolymer vesicles were concentrated on vesicles with homogeneous hydrophobic membranes, *i.e.*, the membrane-forming block consists of a single component.[26,38–41] Vesicles with inhomogeneous hydrophobic membranes were seldom considered in the studies of vesicle disassembly. The inhomogeneous hydrophobic membranes can be constructed by membrane-forming blocks that consist of two different components. For instance, Brannan and Bates once reported an AB-CA-type of vesicles with the inhomogeneous hydrophobic membrane formed experimentally by poly(ethylene oxide)-poly(styrene)-poly(butadiene)-poly (ethylene oxide) (PEO-PS-PB-PEO) tetrablock terpolymers, in which the membrane-forming block is composed of PS-PB blocks.[42] The vesicles self-assembled by the PEO-PS-PB-PEO tetrablock terpolymers possess an interesting asymmetric characteristic, that is the inner layer of the inhomogeneous hydrophobic membrane is always occupied by the PB block under a certain condition. Such asymmetric characteristic endows those vesicles with unique application values in the field of drug delivery. For example, many potential technical applications of reconstitutions of cell membranes inserted with proteins depend on the correct orientation of the protein, and the correct orientation of the inserted protein further depends on the asymmetric property of the vesicle membrane.[43] However, to our knowledge, the disassembly behavior of this kind of asymmetric vesicles has not been reported before. The external stimuli-triggered disassembly behavior of such vesicles is therefore unclear so far. In this work, we implemented the Monte Carlo simulation method to study the disassembly behavior of asymmetric vesicles formed by the ABCA tetrablock copolymers in solvents selective for block A. The hydrophobicity of block C was tuned to mimic the hydrophobic-hydrophilic transition triggered by external stimuli (such as pH, temperature, light, *etc*.). In this way, the disassembly behavior of the initial asymmetric ABCA tetrablock terpolymer vesicle as well as the reversibility of the disassembly processes were studied systemically.

https://doi.org/10.1007/s10118-026-3778-3

MODEL AND METHODS

Simulation Model

The Lattice Monte Carlo simulation method was employed in this paper. The system is embedded in a simple cubic lattice of volume $V = L \times L \times L$ with $L = 50$. Periodic boundary conditions are imposed in all three directions. The polymer concentration in the simulation box is fixed at $c_P = 7\%$, and the rest lattice sites are occupied by solvent molecules. Each monomer occupies one lattice site, and the monomers are self-avoiding. The single-site bond fluctuation model[44–46] is used, and the permitted bond length is 1 and $\sqrt{2}$. The chain conformation evolution is achieved through monomer motions. Each step of the monomer motion is generated through a microrelaxation model, which is highly efficient in relaxing local chain conformation on the lattice[47] and is suitable for dynamic process studies.[48,49] The microrelaxation model is defined as follows: a monomer is randomly chosen to exchange with one of its 18 nearest neighbors. If the neighbor is a solvent molecule, then the exchange is attempted. If the exchange does not violate the bond length restriction, the exchange is allowed. This process constitutes a single movement. If the exchange would break two chain connections, it is disallowed. If the exchange creates a single break in the chain, the solvent will continue to exchange with subsequent monomers along the chain until reconnection of the links occurs. The acceptance or rejection of a monomer motion is further governed by the Metropolis rule:[50] if the energy change ΔE is negative, the exchange is accepted. Otherwise, the exchange is accepted with a probability of $p = \exp[-\Delta E/(k_B T)]$, where $\Delta E = \sum_{ij} \Delta N_{ij} \varepsilon_{ij}$ is the energy change caused by the attempted move; ΔN_{ij} is the number difference of the nearest neighbor pairs between components i and j before and after the movement, where i, j = A, B, C and S (solvent), respectively; ε_{ij} is the reduced interaction energy between components i and j; and k_B is the Boltzmann constant and assumed to be 1 in the whole simulation. The parameter T is the reduced temperature.

Construction of the Initial ABCA Tetrablock Terpolymer Vesicle

The asymmetric vesicle formed by ABCA tetrablock terpolymers is the main focus in the current study. The formation conditions of such asymmetric vesicles have been systematically studied in our previous simulation works.[51,52] Based on our previous works, the reduced interaction energies between different components in the system are set as follows: the interaction energies among different blocks in the terpolymers are set as positive to mimic the incompatibilities between different species, *i.e.*, $\varepsilon_{AB} = \varepsilon_{AC} = 1.0$, and $\varepsilon_{BC} = 2.0$. The interaction energy between hydrophilic block A and solvent S is set as $\varepsilon_{AS} = -1.0$, the interaction energy between hydrophobic block B and solvent S is set at $\varepsilon_{BS} = 2.6$, while the interaction energy between block C and solvent S is set as $\varepsilon_{CS} = 3.5$, according to the amphiphilic nature of the terpolymer concerned in this study. All other self-interaction energies between the same components, *i.e.*, ε_{AA}, ε_{BB}, ε_{CC}, and ε_{SS}, are set as 0. To ensure the formation of a regular and stable vesicle, the annealing method is implemented, and the detailed information on the annealing process can be found in our previous work.[52] The simulation time is measured by Monte Carlo step (MCS), and in one MCS, on average, each monomer has attempted one exchange move. For the convenience of statistics, a larger simulation time unit (ts) has been introduced, *i.e.*, 1 ts = 7000 MCS.

Based on the aforementioned parameter settings, the $A_2B_7C_5A_2$ tetrablock terpolymer system started to self-assemble from a homogenous state (Fig. 1a), and finally formed a spherical aggregate (Fig. 1b) when the whole annealing process was done. The cross-section shown in Fig. 1(b1) demonstrates the hollow structure in the aggregate, which proves that the aggregate shown in Fig. 1(b) is a vesicle. The snapshots of hydrophobic parts shown in Figs. 1(b2)–1(b4) indicate that the outer and inner layers of the vesicle membrane are occupied by blocks B and C respectively, which clearly shows the asymmetric characteristic of the vesicle membrane. In order to further confirm the structure of this asymmetric vesicle, the variations of densities of different components in the vesicle with the radii around the mass center of the vesicle were calculated and shown in Fig. 1(c). From the peak positions on each variation curve, it can be seen that the center of the vesicle is filled with solvent molecules, the shorter hydrophobic blocks C distribute in the inner layer, the longer hydrophobic blocks B distribute in the outer layer, and the hydrophilic blocks A distribute in the innermost and the outermost layers of the vesicle, respectively. Fig. 1(c) further proves that the vesicle formed by $A_2B_7C_5A_2$ tetrablock terpolymers is a well-defined asymmetric vesicle, and therefore

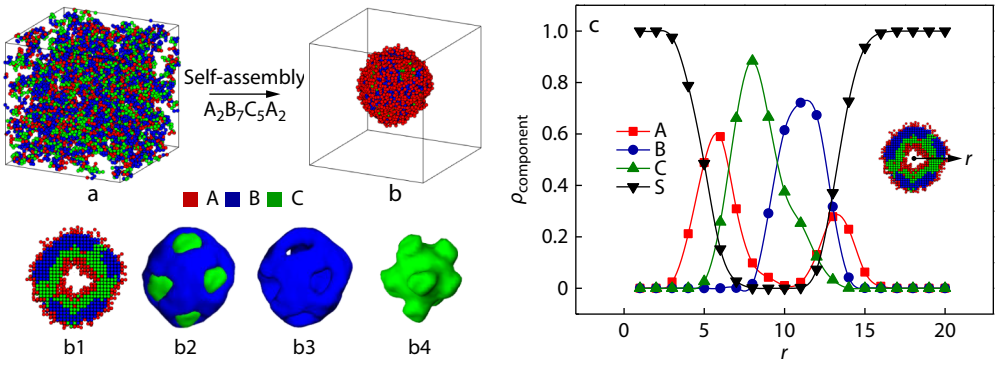

Fig. 1 (a) Homogeneous state of the $A_2B_7C_5A_2$ tetrablock terpolymers; (b) Overall morphology of the vesicle self-assembled by the $A_2B_7C_5A_2$ tetrablock terpolymers from the homogeneous state shown in (a); (c) Variations of densities of components A, B, C and solvents (S) with the radii (r) around the mass center of the vesicle shown in (b). (b1–b4) are the cross-section, the whole hydrophobic parts, and the hydrophobic parts formed by blocks B and C in the vesicle shown in (b).

https://doi.org/10.1007/s10118-026-3778-3

in this paper, the asymmetric vesicle shown in Fig. 1(b) was selected as the initial state to investigate its disassembly behavior induced by the external stimuli-triggered hydrophobic-hydrophilic transition of block C.

RESULTS AND DISCUSSION

In this section, the hydrophobicity of block B remains unchanged ($\varepsilon_{BS}=2.6$), while the hydrophobicity of block C (ε_{CS}) decreases from $\varepsilon_{CS}^{0}=3.5$ (the initial hydrophobicity of block C) to a series of smaller values ε_{CS}^{t} (which varies in the range of 3.0 to 0.0) to mimic the hydrophobicity changes of block C triggered by the external stimuli. The purpose is to investigate the effect of the hydrophobic-hydrophilic transition of block C on the disassembly behavior of the asymmetric $A_2B_7C_5A_2$ tetrablock terpolymer vesicles.

Disassembly Behavior of the Asymmetric Vesicle Triggered by the Hydrophobic-Hydrophilic Transition of Block C

Fig. 2 shows the aggregate morphologies evolved from the $A_2B_7C_5A_2$ tetrablock terpolymer asymmetric vesicles (Fig. 2a) when the hydrophobicity of block C was changed to different values of ε_{CS}^{t} after a sufficiently long simulation time (t>3000 ts). From Fig. 2, it can be seen that when the hydrophobicity of block C is decreased to $\varepsilon_{CS}^{t}=3.0$, the initial asymmetric vesicle structure cannot be maintained anymore and disassembles into Janus lamella (Fig. 2b), in which blocks B and C are located on the two sides of the lamella, respectively. It is found that the Janus lamella shown in Fig. 2(b) always, to some extent, slightly bends towards the side formed by block C, which can be seen from the cross-section of the lamella shown in Fig. 2(b1). This is mainly because at this moment, the hydrophobicity of block C ($\varepsilon_{CS}^{t}=3.0$) is stronger than that of block B (which is fixed at $\varepsilon_{BS}=2.6$). The stronger hydrophobicity causes blocks C to stack more tightly in the Janus lamella, forming a slightly smaller inner surface of the curved lamella. When ε_{CS}^{t} is decreased to 2.5, which is close to that of block B, an almost planar Janus lamella (Fig. 2c1) is formed. Further decreasing the hydrophobicity of block C to $\varepsilon_{CS}^{t}=2.0$ will make the hydrophobicity of block C becomes weaker than that of block B, which makes block B aggregates more tightly than block C. Therefore, Janus lamella that always bends towards the side formed by block B is observed in this case (Fig. 2d1). In addition to the observation of the Janus lamella with different bending mode, another interesting phenomenon was observed, that is, when ε_{CS}^{t} is decreased to 1.5, another kind of asymmetric vesicle (Fig. 2e) was formed. It is worth noting that compared to the original asymmetric vesicle shown in Fig. 2(a), this asymmetric vesicle has a reversed membrane structure. In order to clearly demonstrate the asymmetric vesicle structure shown in Fig. 2(e), the hydrophobic parts formed by blocks B and C are drawn separately and shown in Figs. 3(a) and 3(b). It can be seen that due to the hydrophobicity difference between blocks B and C, the blocks B with stronger hydrophobicity form a closed membrane located on the inner side, while the blocks C with weaker hydrophobicity form a cage-like membrane located on the outer surface of the vesicle. The variations of the component densities ($\rho_{component}$) with the radii (r) around the mass center of the vesicle can further prove this asymmetric structure (Fig. 3c). This simulation result indicates that the reverse of the asymmetric vesicle membrane structure can be achieved by the external stimuli-triggered hydrophobicity changes. Besides those aggregates with novel asymmetric structures, toroid micelle (Fig. 2f) can be obtained when further decrease ε_{CS}^{t} to 1.0. The core of the toroid is composed of blocks B (Fig. 2f1), while the blocks C with weaker hydrophobicity form irregular structures covering its surface. Further decreasing ε_{CS}^{t}, blocks C cannot form dense structures anymore, and some conventional micelles, *i.e.*, ring-like micelle (Fig. 2g) and cylindrical micelle (Fig. 2h) can be obtained by the disassembly of the initial asymmetric vesicles formed by the $A_2B_7C_5A_2$ tetrablock terpolymers.

Fig. 2 indicates that various novel aggregates can be obtained through the disassembly of the initial ordered asymmetric $A_2B_7C_5A_2$ tetrablock terpolymer vesicle (*i.e.*, Fig. 2a). An interesting issue is whether those ordered aggregates shown in Fig. 2 can be obtained through the traditional self-assembly process from homogeneous states of $A_2B_7C_5A_2$ tetrablock terpolymers under the same parameter conditions. For this purpose, a homogeneous state of the $A_2B_7C_5A_2$ tetrablock terpolymers (Fig. 4a) was selected as the initial state. Starting from this homogeneous state, a series of simulations with the

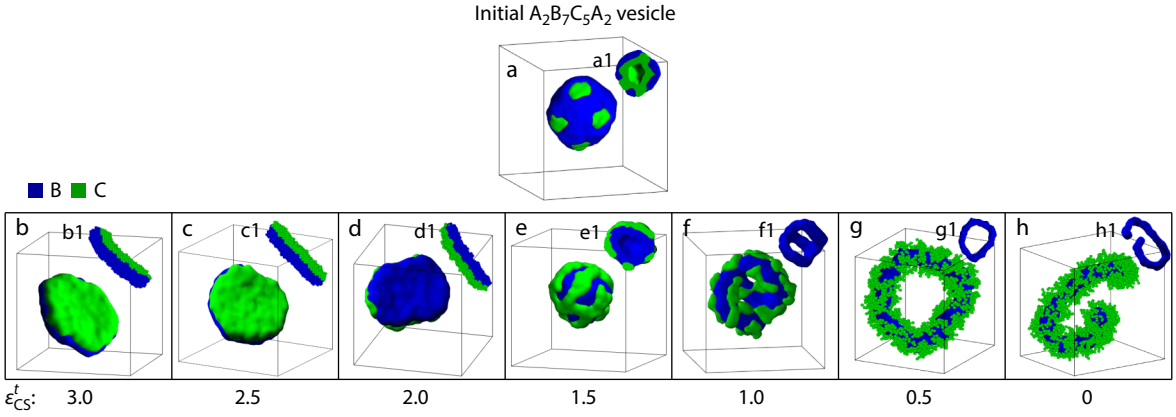

Fig. 2 (a) The initial asymmetric $A_2B_7C_5A_2$ tetrablock terpolymer vesicle. (b–h) Morphologies of the aggregates evolved from the asymmetric vesicle shown in (a) with different hydrophobicities of block C (ε_{CS}^{t}). (a1–e1) are cross-sections of (a–e). (f1–h1) are the hydrophobic parts formed by blocks B in (f–h). For clarity, only hydrophobic parts formed by blocks B and C are drawn in this figure.

https://doi.org/10.1007/s10118-026-3778-3

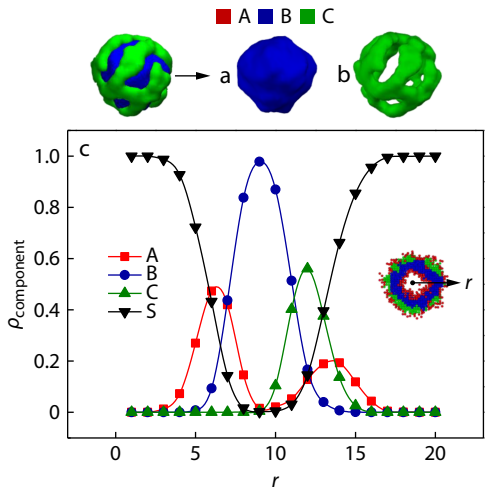

Fig. 3 (a, b) The hydrophobic parts formed by blocks B and C in the vesicle shown in Fig. 2(e); (c) Variations of densities of components A, B, C and solvents (S) with the radii (r) around the mass center of the vesicle shown in Fig. 2(e).

same ε_{CS} settings as those in Fig. 2 were performed, and the simulation results obtained after a sufficiently long simulation time (*i.e.*, t>3000 ts) are shown in Fig. 4. From Figs. 4(b)–4(f), it can be seen that the tetrablock terpolymer systems with various ε_{CS} mainly self-assemble into many small hamburger-like spheres in which the layer formed by block B located in between the layers formed by block C. When $\varepsilon_{CS} \le 0.5$, traditional spherical micelles (where the cores are formed by blocks B) with smaller sizes are observed (Figs. 4g and 4h). Compared with Fig. 2, it can be seen that for the same ε_{CS}, the morphologies and structures of the aggregates obtained through the self-assembly starting from the homogeneous states are significantly different from those obtained through the disassembly starting from the initial ordered vesicles. The above results indicate that for the same block copolymer system, the novel microphase separation structures formed from the vesicle state through disassembly processes shown in Fig. 2 cannot be obtained through the traditional self-assembly method. This means that the formation of ordered aggregates of the tetrablock terpolymers in selective solvents has a strong initial state dependence. It is worth noting that recently, the disassembly of block copolymer vesicles induced by the hydrophobic-hydrophilic transition of one constituent block in a diblock copolymer has been successfully achieved by Yu *et al.*[26]. *Via* the introduction of 4-hydroxyazobenzene (Azo–OH) onto the P4VP block of the PS-P4VP diblock copolymer, the hydrophilicity of P4VP block can be tuned in a controllable manner by UV irradiation. The originally stable polymeric vesicles formed by PS-P4VP(Azo–OH) can transform into various micelles, including toroid and cylinder, under UV irradiation. Interestingly, the strong initial state dependence was also found in their experiments. That is, the toroid micelles obtained from the UV triggered morphological transformation pathway cannot be obtained through the traditional self-assembly pathway.

Dynamic Pathways of the Morphological Transformation from the Initial Asymmetric Vesicle to the Reversed Asymmetric Vesicle

It is important to investigate the dynamic pathways of the disassembly processes of vesicles because it is crucial for realizing applications of vesicles such as drug delivery, controlled release, fabrication of novel ordered aggregates, and so on. Therefore, in this subsection, the disassembly process from the initial asymmetric vesicle (Fig. 2a) to the interesting reversed asymmetric vesicle (Fig. 2e) was studied in details.

Fig. 5 shows the morphologies of the aggregates observed at different simulation times after changing the hydrophobicity of block C in the initial vesicle from $\varepsilon_{CS}^{0} = 3.5$ to $\varepsilon_{CS}^{t} = 1.5$. From the morphological changes of the hydrophobic parts formed by block C, it can be seen that due to the sudden decrease in the hydrophobicity of block C, the originally closed bumpy inner layer (Fig. 5a1) suddenly breaks, and migrates towards the outer surface of the vesicle (Figs. 5b and 5b1). As the simulation time increases, the broken layer further disassembles into multiple strips wrapping outside the area formed by blocks B (Figs. 5c–5g, 5c1–5g1). As for the hydrophobic parts formed by blocks B, the pores in the originally perforated layer gradually merged with increasing simulation time, which leads to the formation of a series of novel structures, such as the perforated tube (Fig. 5c2), normal tube (Fig. 5d2), and bowl-shaped membrane (Fig. 5e2). Further in-

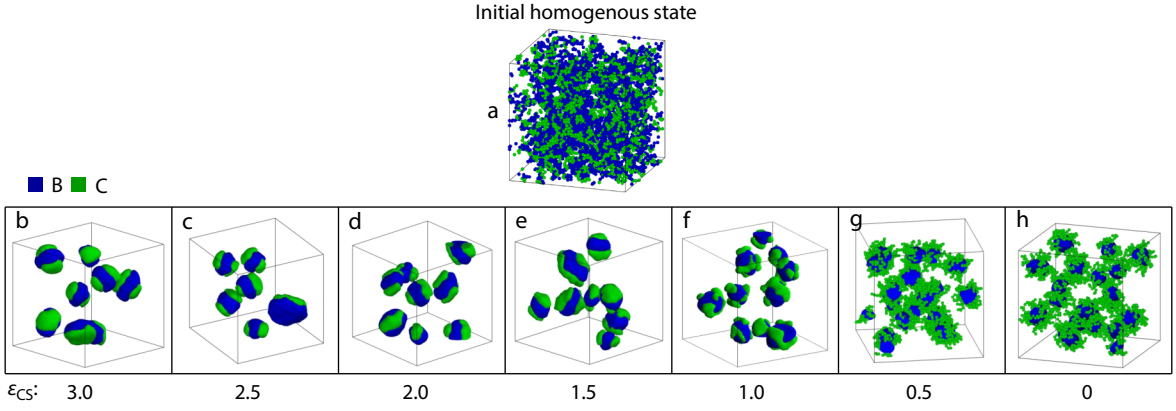

Fig. 4 (a) The initial homogenous solution of $A_2B_7C_5A_2$ tetrablock terpolymers. (b–h) Morphologies of the aggregates evolved from the homogenous state shown in (a) with different hydrophobicities of block C (ε_{CS}). For clarity, only hydrophobic parts formed by blocks B and C are drawn in this figure.

https://doi.org/10.1007/s10118-026-3778-3

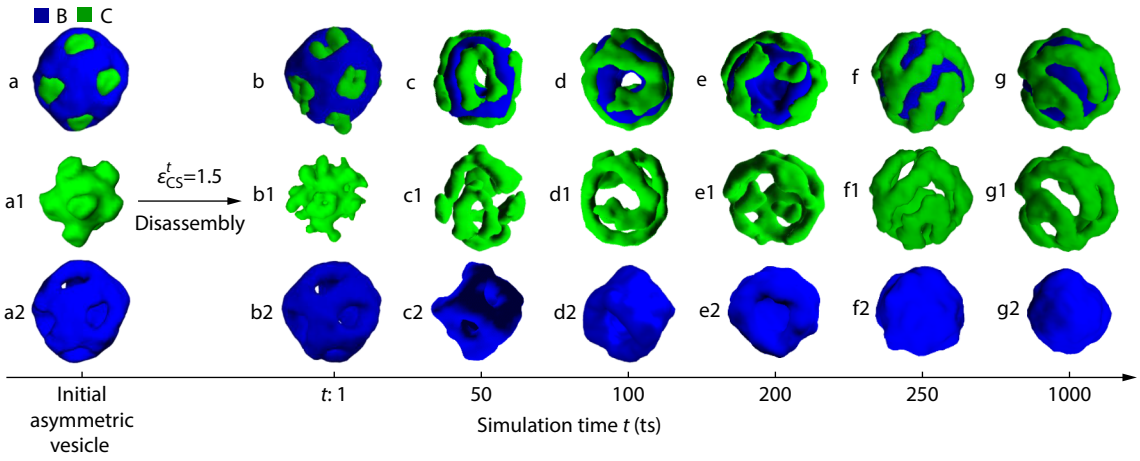

Fig. 5 (a–g) Snapshots at different simulation times showing the pathway of the transformation from the initial asymmetric vesicle to the reversed asymmetric vesicle. (a1–g1) and (a2–g2) are the morphologies of the hydrophobic parts formed by blocks B and C in (a–g), respectively.

creasing the simulation time, the perforated layer finally transformed into a closed spherical membrane (Fig. 5f2), forming the inner layer of the newly formed reversed asymmetric vesicle (Fig. 5f). This transformation process is very fast, *i.e.*, the reversed vesicle is formed at about t = 250 ts (Fig. 5f), and the structure of the vesicle remains almost unchanged with further increasing simulation time (Fig. 5g), which indicates that the newly formed reversed asymmetric vesicle is stable. From the morphological changes of the hydrophobic parts formed by blocks B and C, it can be concluded that the morphological transformation from the initial asymmetric vesicle (Fig. 5a) to the finally formed reversed asymmetric vesicle (Fig. 5g) mainly involves two processes, *i.e.*, the migration of the hydrophobic block C from the inner layer to the outer layer of the vesicle (Figs. 5b–5g), and the fusion of the pores in the perforated layer formed by block B into a closed spherical membrane (Figs. 5b2–5g2).

In addition, according to experimental results in the literature, the external stimuli-triggered hydrophobic-hydrophilic transition rate of a certain block generally have a significant impact on the disassembly behavior of ordered aggregates.[16,26,53–55] Based on this, in addition to the case shown in Fig. 5 that the hydrophobicity of block C (ε_{CS}) was directly changed from the initial value (ε_{CS}^{0} = 3.5) to the target value (ε_{CS}^{t} = 1.5), two different hydrophobicity changing rates were employed, *i.e.*, r_{cs} = 0.05/ts and 0.001/ts. In the case of r_{cs} = 0.05/ts, it takes 40 ts for ε_{CS} to change from 3.5 to 1.5, which corresponds to a relatively fast hydrophobicity changing rate. In the case of r_{cs} = 0.001/ts, it takes 2000 ts for ε_{CS} to change from 3.5 to 1.5, which corresponds to a relatively slow hydrophobicity changing rate. Figs. 6(a) and 6(b) show the morphological transformation processes of the initial asymmetric vesicle under this two different hydrophobicity changing rates. It can be seen that in both cases, the initial asymmetric vesicles will eventually transform into the reversed asymmetric vesicles (Figs. 6a6 and 6b6) similar to the vesicle shown in Fig. 5(g), while the morphological transformation pathways in these two cases are different. In the case of the fast hydrophobicity changing rate (Fig. 6a), the morphological transformation pathway is quite similar to that shown in Fig. 5, *i.e.*, the hydrophobic block C migrates from the inner layer to the outer layer of the vesicle (Figs. 6a1–6a6), while the perforated layer formed by block B fuses into a closed spherical membrane (Figs. 6a1′–6a6′). However, in the case of the slow hydrophobicity changing rate (Fig. 6b), the morphological transformation pathway is totally different. From Fig. 6(b), it can be seen that a small pore in the vesicle membrane is formed at first when the simulation time is t = 500 ts (Fig. 6b1). As the simulation time increases, the small pore becomes larger, and a bowl-shaped lamella with its inner side formed by block C is formed (Figs. 6b2 and 6b2′). As the simulation time increases to t = 1000 ts, the bowl-shaped lamella becomes flat and transforms into a plane Janus lamella (Figs. 6b3 and 6b3′). It should be noted that at this simulation time, the value of ε_{CS} decreases to 2.5, which is approximately equal to the value of ε_{BS} (ε_{BS} = 2.6). This is why a very flat Janus lamella with blocks B and C located on either side can be observed. As the simulation time increases to t = 2000 ts, ε_{CS} further decreases to the value that is smaller than ε_{BS}, and due to the stronger hydrophobicity of block B, the plane Janus lamella tend to bend toward the side formed by block B (Figs. 6b4 and 6b4′). Further increasing the simulation time, a reversed bowl-shaped lamella with its inner side formed by block B (Figs. 6b5 and 6b5′) is formed, and this reversed bowl-shaped lamella eventually bends and closes into the reversed asymmetric vesicle (Figs. 6b6 and 6b6′) at t = 8000 ts. This simulation results indicate that the hydrophobicity changing rate of the responsive block C does have a significant effect on the disassembly pathway from the initial asymmetric vesicle to the reversed asymmetric vesicle.

To further reveal the difference in the morphological transformation pathways shown in Fig. 6 at a microscopic level, the simulation results showing the variation of the mean-square end-to-end distance of the hydrophobic blocks constructed by blocks B and C ($\langle R_{BC}^{2} \rangle$) and the interaction energy of the system (E) with simulation time (t) under the fast and slow hydrophobicity changing rates are given in Fig. 7. In the case of fast-changing rate with r_{cs} = 0.05, when the hydrophobicity of block C decreases rapidly from 3.5 to 1.5, an expected rapid decrease in the interaction energy of the system was observed within 300 ts. The initial asymmetric vesicle (Fig. 7a1) transformed into the tube (Fig. 7a2) in this time period.

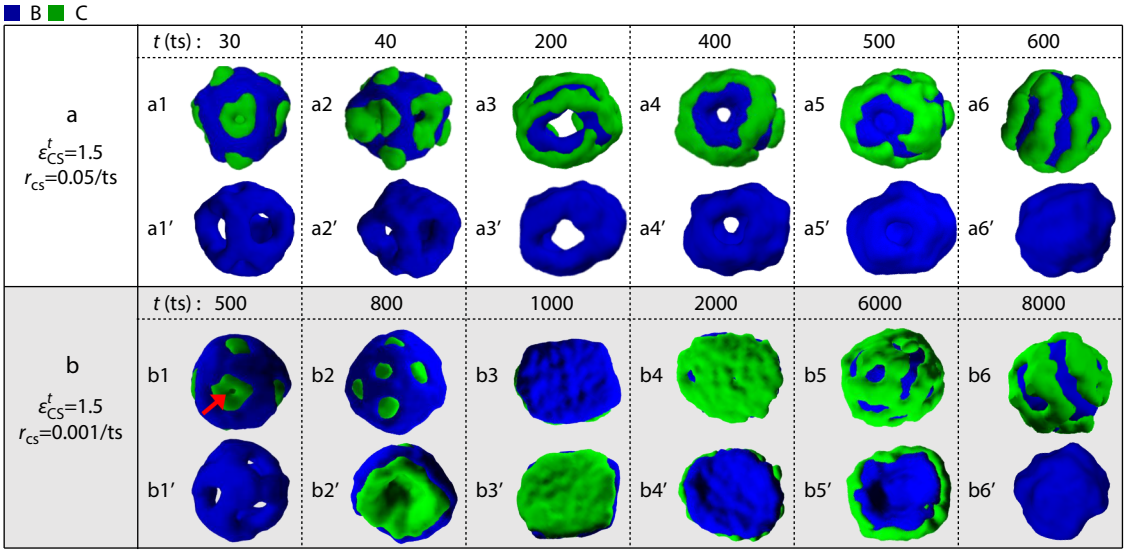

Fig. 6 The transformation pathways from the initial asymmetric vesicle to the reversed asymmetric vesicle when the hydrophobicity changing rates (r_{cs}) are r_{cs} = 0.05/ts (a) and r_{cs} = 0.001/ts (b), respectively; (a1–a6) and (b1–b6) are the overall morphologies of the hydrophobic parts at different simulation times; (a1′–a6′), (b1′) and (b6′) are the morphologies of the hydrophobic parts formed by block B; (b2′–b5′) are the overall morphologies of the hydrophobic parts from different view angles. The red arrow in (b1) shows the location of the pore on the vesicle membrane.

At the same time, it can be seen that $\langle R_{BC}^2 \rangle$ undergoes a rapid increase from 36 to 40. It should be noted that the $\langle R_{BC}^2 \rangle$ value of the unperturbed $A_2B_7C_5A_2$ tetrablock terpolymer chains is about 29. An increase of $\langle R_{BC}^2 \rangle$ from 36 to 40 indicates that a rapid stretching of the polymer chains occurs, which leads to an increase in the penalty of the conformational entropy of the polymer chains. It is worth mentioning that the penalty of the conformational entropy of the polymer chains does not increase spontaneously, it is caused by the decrease in the interaction energy of the system, which means that the morphological transformation from the initial asymmetric vesicle (Fig. 7a1) to the tube (Fig. 7a2) is an energy-driven process when t < 300 ts. To relax the chain stretching, hence to relieve the entropic penalty, the tube (Fig. 7a2) gradually transforms into the reversed asymmetric vesicle (Fig. 7a3) with the decrease in $\langle R_{BC}^2 \rangle$ during the time period of 300 ts<t < 600 ts. It should be noted that during this time period, when $\langle R_{BC}^2 \rangle$ decreases, the interaction energy of the system is almost unchanged, meaning that the morphological transformation from the tube (Fig. 7a2) to the reversed asymmetric vesicle (Fig. 7a3) is an entropy-driven process. Thereafter, $\langle R_{BC}^2 \rangle$ and E, as well as the aggregate structure (*i.e.*, the reversed asymmetric vesicle) (Fig. 7a4) remain unchanged with further increasing simulation time. In the case of slow-changing rate with r_{cs} = 0.001 shown in Fig. 7(b), it is seen that the interaction energy of the system decreases, while $\langle R_{BC}^2 \rangle$ increases within 1200 ts. During this time period, the initial asymmetric vesicle (Fig. 7b1) transforms into the plane Janus lamella (Fig. 7b2). The same as the case of fast-changing rate, this process is also an energy-driven process. Subsequently, to relieve the entropic penalty caused by the chain stretching, the system undergoes an entropy-driven process, during which the plane Janus lamella changes slowly with time firstly to the bow-shaped lamella (Figs. 7b3 and 7b4), and then to the final reversed asymmetric vesicle (Figs. 7b5 and 7b6). In general, no matter the hydrophobicity changing rate of the systems is fast or slow, both systems will undergo an energy-driven process first, then followed by an entropy-driven process during the structure transformation from the initial asymmetric vesicle to the reversed asymmetric vesicle. However, comparing Figs. 7(a) and 7(b), we notice that when the hydrophobicity of block C is changed rapidly, the chain stretching relaxes only once, *i.e.*, the relaxation of the chain stretching occurs when 300 ts<t < 600 ts, and the interaction energy of the system remain unchanged in this chain relaxation process (Fig. 7a). While when the hydrophobicity of block C is changed very slowly, the polymer chains will become much more stretched at the end of the energy-driven process (which can be deduced from the high value of $\langle R_{BC}^2 \rangle$ at t = 1200 ts shown in Fig. 7b), and the more stretched polymer chains exhibit two relaxation processes, which appears at 1200 ts<t < 3600 ts and 7000 ts<t < 8000 ts, respectively.

Reversibility of the Disassembly of the Initial Asymmetric Vesicles

Whether the disassembly of the initial vesicles is reversible is also an important issue concerned in experiments.[25,26] Therefore, in this subsection, in order to test the reversibility of the disassembly, *i.e.*, to test whether the $A_2B_7C_5A_2$ tetrablock terpolymer aggregates formed at different ε_{CS}^{t} shown in Fig. 2 can be transformed back to the initial asymmetric vesicles *via* changing the hydrophobicity of block C back to ε_{CS}^{0} = 3.5, three typical $A_2B_7C_5A_2$ tetrablock terpolymer aggregates (Figs. 2b, 2e and 2h) were selected, and two hydrophobicity changing rates, *i.e.*, the direct-changing rate (the hydrophobicity of block C is directly changed from ε_{CS}^{t} back to 3.5), and the slow-changing rate with r_{cs} = 0.001 are implemented. Fig. 8 shows the morphologies obtained when the hydrophobicity of block C is changed from typical ε_{CS}^{t} (Figs. 8a–8c) back to ε_{CS}^{0} = 3.5 after a sufficiently long simulation time (t > 10^4 ts). For the Janus lamella (Fig. 8a) and the reversed asymmetric vesicle (Fig. 8b), it can be seen that the

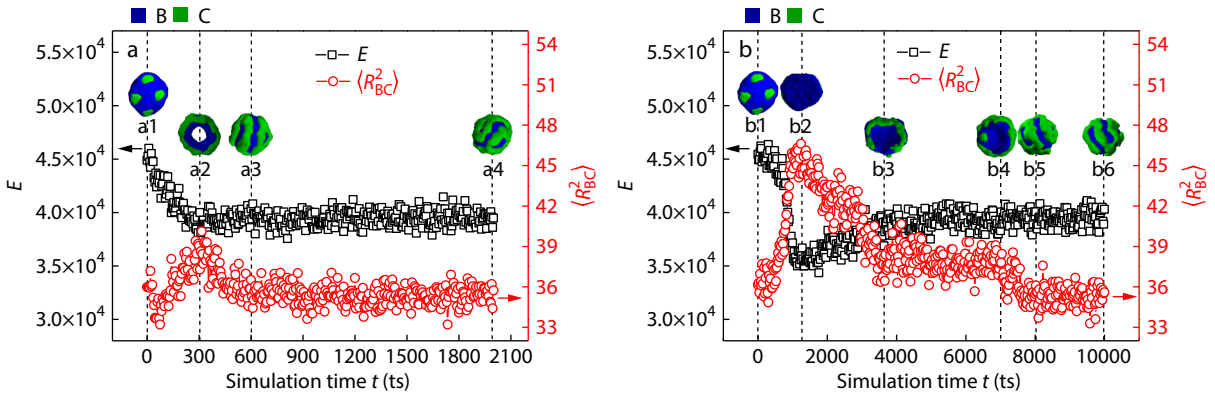

Fig. 7 Variations of the mean-square end-to-end distance of the hydrophobic blocks constructed by blocks B and C ($\langle R^2_{BC}\rangle$) and the interaction energy of the system (E) with simulation time (t) under different hydrophobicity changing rates (r_{cs}). (a) $r_{cs}=0.05$, (b) $r_{cs}=0.001$. For clarity, corresponding morphologies of the hydrophobic blocks at different simulation time are given in (a1–a4) and (b1–b6). (a1) $t=0$ ts, (a2) $t=300$ ts, (a3) $t=600$ ts, (a4) $t=2000$ ts; (b1) $t=0$ ts, (b2) $t=1200$ ts, (b3) $t=3600$ ts, (b4) $t=7000$ ts, (b5) $t=8000$ ts, (b6) $t=10000$ ts.

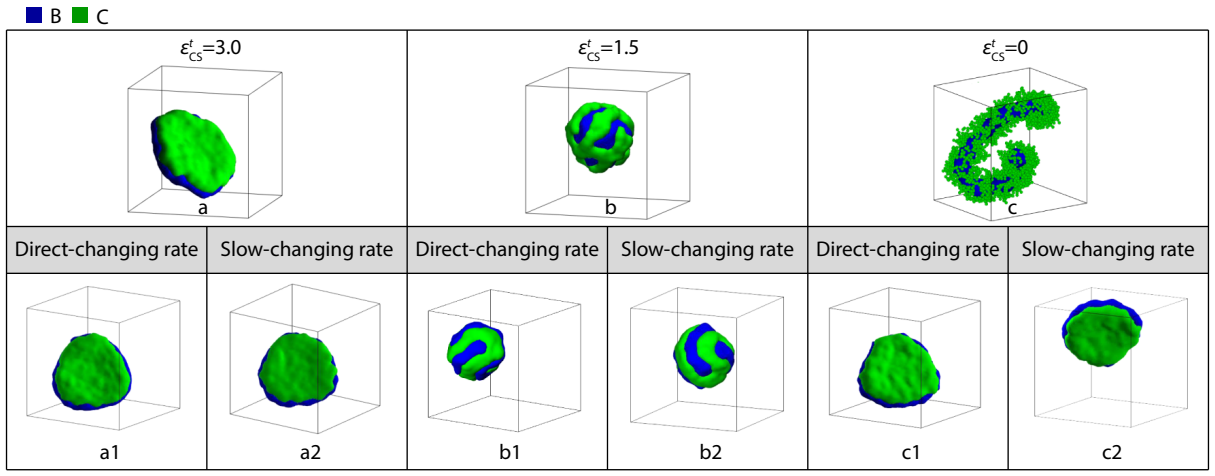

Fig. 8 (a–c) Three typical aggregates with different ε^t_{CS} obtained from the disassembly of the initial asymmetric vesicle. (a1–c1) and (a2–c2) Morphologies of the aggregates evolved from (a–c) when the hydrophobicity of block C is changed from ε^t_{CS} back to 3.5 with direct- and slow-changing rate ($r_{cs}=0.001$), respectively. For clarity, only hydrophobic parts formed by blocks B and C are drawn in this figure.

aggregate morphologies remain unchanged (Figs. 8a1, 8a2, 8b1 and 8b2) when ε^t_{CS} is changed back to the initial value $\varepsilon^0_{CS}=3.5$, no matter the changing rate is fast or slow. For the cylindrical micelle (Fig. 8c), the Janus lamella (Figs. 8c1 and 8c2) was obtained in the current simulations after ε^t_{CS} is changed back to the value of 3.5. In general, the simulation results shown in Fig. 8 indicates that the obtained morphologies disassembled from the initial asymmetric vesicles by decreasing the hydrophobicity of block C cannot be transformed back to the initial vesicles by increasing the hydrophobicity of block C, which means that the disassembly of the initial asymmetric vesicles is irreversible. This phenomenon can be explained from the angle of energy. When the interaction between block C and solvent S (*i.e.*, the hydrophobicity of block C) is decreased from the initial $\varepsilon^0_{CS}=3.5$ to a certain lower value ε^t_{CS}, the free energy of the system will decrease consequently. Taking the reversed asymmetric vesicle as an example, it can be seen from Fig. 7 that when the hydrophobicity of block C is decreased from the initial value $\varepsilon^0_{CS}=3.5$ to the lower value $\varepsilon^t_{CS}=1.5$, the interaction energy of the system (E) apparently decreases from about 4.6×10^4 to 4.0×10^4 in both cases, whereas the mean-square end-to-end distance values of the initial asymmetric vesicle and the reversed vesicle are almost the same (*i.e.*, $\langle R^2_{BC}\rangle \approx 36$). Therefore, the transformation from the initial asymmetric vesicle to the reversed asymmetric vesicle is a process that decreases the free energy of the system. This means that the reverse process of the disassembly (*i.e.*, the transformation from the reversed asymmetric vesicle to the initial asymmetric vesicle) will be a process accompanied by an increase in the free energy of the system. It should be noted that Ye and Yu *et al.*[25,26] reported a light-triggered reversible transformation from AB diblock copolymer vesicle to cylindrical micelle in experiments, which is different from our simulation results shown in Fig. 8. Besides the different types of block copolymers adopted in their experiments and in our simulations, this inconsistency between the experiments and the current work can also be explained from the angle of energy. It is known that the assembly/disassembly of a polymer system is mainly a thermodynamically driven process, during which some energy barriers have to be overcome. In experiments, the morphological evolution generally occurs under a stirring condition.[25,26] The imposed stirring in experiments can provide an extra, other than the thermodynamic, driving force

to help the aggregates overcome energy barriers to achieve the transformation between different morphologies, especially in a transformation process that leads to an increase in energy. As mentioned above, the transformation from the reversed asymmetric vesicle to the initial asymmetric vesicle is a process accompanied by an increase in the free energy of the system, which needs to overcome some energy barriers to achieve. However, in our simulations, except for the thermodynamic driving force, no extra driving force was introduced in our simulations to overcome the energy barriers during the morphological transition. Therefore, the reverse process can hardly be achieved spontaneously without any external disturbance. This may be a reason why the disassembly of the asymmetric vesicle studied in this work is irreversible.

Universality of the Current Study

In the current work, we have taken a tetrablock terpolymer chain with a fixed chain length and composition as an example to investigate the disassembly behavior of the asymmetric vesicles formed by $A_2B_7C_5A_2$ tetrablock terpolymers. The selection and optimization of the total chain length and the length of each block A are based on the experimental work reported by Brannan *et al*.[42] More details for the length selection were provided in our previous simulation work.[52] The influence of different total chain lengths and block ratios (*e.g.*, B/C length ratio) on the disassembly behavior has not been explored. However, for the effect of B/C length ratio, it can be seen from our previous simulation works[51,52] that as the B/C length ratio increases from 7:5 to 8:4, the variations of self-assembly morphologies with the change in ε_{cs} are quite similar. Analogously, at different B/C length ratios, the disassembly morphologies of the vesicles with the change in ε_{cs} should also be similar on the whole. For the effect of the total chain length, Discher and Eisenberg have pointed out that the molecular weight (equivalent to the chain length) of polymer chains mainly affects the fluidity of molecular chains.[56] For example, a higher molecular weight may slow down the rearrangement of polymers within aggregates and delay the formation of the final morphology and structure of aggregates. Therefore, in our simulation works, the total chain length will mainly affect the time required for the system to evolve from one morphology to another. In conclusion, as far as the current ABCA terpolymer system is concerned, our simulation results have a certain degree of universality.

CONCLUSIONS

The disassembly behavior of the ABCA tetrablock asymmetric vesicles induced by the hydrophobic-hydrophilic transition of block C was systematically studied using Monte Carlo simulation. By gradually decreasing the hydrophobicity of block C, the initial ABCA asymmetric vesicles were disassembled in the order of Janus lamella, reversed asymmetric vesicle, toroid micelle, ring-like micelle and cylindrical micelle. These aggregates disassembled from the initial asymmetric vesicle state cannot be obtained through the traditional self-assembly method from homogeneous states of the ABCA tetrablock terpolymers under the same conditions. The simulation results show that although the formation of the reversed asymmetric vesicles is independent of the hydrophobicity changing rate of block C, the hydrophobicity changing rate has a significant effect on the disassembly pathway of the initial asymmetric vesicle. It is also found that the system will undergo an energy-driven process first, then followed by an entropy-driven process during the disassembly from the initial asymmetric to the reversed asymmetric vesicles. Furthermore, the simulation results indicate that because the reverse process of the disassembly of the initial asymmetric vesicles is a process of increasing the free energy of the system, the disassembly behavior of the initial ABCA asymmetric vesicles is irreversible. The present work not only deepens the understanding about the disassembly behavior of the inhomogeneous vesicles formed by the ABCA tetrablock terpolymers, but also provides new clues for fabrications of structure-controlled polymer aggregates.

Conflict of Interests

The authors declare no interest conflict.

Data Availability Statement

Data supporting the findings of this study can be provided by contacting the corresponding author.

ACKNOWLEDGMENTS

This work was financially supported by the National Natural Science Foundation of China (No. 52433001), the Scientific Research Fund of Liaoning Provincial Education Department (No. JYTMS20231437), the Talent Scientific Research Fund of Liaoning Petrochemical University (Nos. 2019XJJL-014 and 2019XJJL-015).

REFERENCES

1 Zhang, Y. N.; Han, Y. L.; Li, J. W.; Shi. T. F. Perforation dynamics and directional motion of Janus vesicles under the coupled effects of flow and electric fields. *Chinese J. Polym. Sci.* **2025**, *43*, 1939−1949.
2 Xu, Q. R.; Wang, Y. W.; Zheng, Y.; Zhu, Y. L.; Li, Z. F.; Liu, Y.; Ding, M. M. Polymersomes in drug delivery-from experiment to computational modeling. *Biomacromolecules* **2023**, *25*, 2114−2135.
3 Zhou, J. W.; Zou, M. H.; Qiu, X. D.; Wang, R. Co-assembly of amphiphilic triblock copolymers with DNA-polymer targeting ligands in solution. *Soft Matter* **2025**, *21*, 5764−5772.
4 Zhou, J. W.; Tang, H.; Wang, R. Co-assembly of amphiphilic triblock copolymers with nanodrugs and drug release kinetics in solution. *J. Phys. Chem. B* **2024**, *128*, 2841−2852.
5 Gao, Y. N.; Gao, C. C.; Fan, Y. R.; Sun, H.; Du, J. Z. Physically and chemically compartmentalized polymersomes for programmed delivery and biological applications. *Biomacromolecules* **2023**, *24*, 5511−5538.
6 Xu, X. F.; Pan, C. Y.; Zhang, W. J.; Hong, C. Y. Polymerization-induced self-assembly generating vesicles with adjustable pH-responsive release performance. *Macromolecules* **2019**, *52*, 1965−1975.
7 Gong, H. Y.; Chen, Y. G.; Yu, X. S.; Xiao, H.; Xiao, J. P.; Wang, Y.; Shuai. X. T. Co-delivery of doxorubicin and afatinib with pH-responsive polymeric nanovesicle for enhanced lung cancer therapy. *Chinese J. Polym. Sci.* **2019**, *37*, 1224−1233.

Graphical Abstract

Effect of External Stimuli-triggered Hydrophobic-Hydrophilic Transition on the Disassembly of ABCA Tetrablock Asymmetric Vesicles: a Monte Carlo Simulation Study

Yan-Qi Zong, Jie Cui, and Yuan-Yuan Han

Liaoning Petrochemical University

Monte Carlo (MC) simulations show that changes in block hydrophobicity can induce the disassembly of ABCA tetrablock asymmetric vesicles, resulting in various ordered structures that are difficult to form *via* traditional self-assembly.

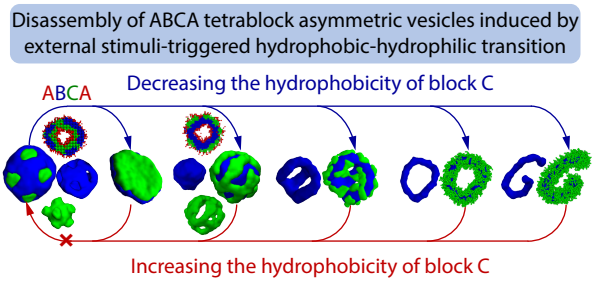

Chinese J. Polym. Sci., 2026 *https://doi.org/10.1007/s10118-026-3778-3*

8 Wang, Z. D.; Peng, C.; Zheng, Y.; Zhang, Y. W.; Xu, T. R.; Yan, J. Y.; Zhou, Y. Q.; Liu, Y.; Xie, H. X.; Wang, C.; Tan, H.; Fu, Q.; Ding, M. M.. Enzyme-inspired nanoreactor containing light-controlled "trojan horse" for redox-hypersensitive drug delivery. *Adv. Funct. Mater.* **2023**, *33*, 2214899.
9 Hu, W.; Su, Y. W.; Jiang, Y. K.; Fan,W. D.; Cheng, S. Y.; Tong, Z. Z.; Cen, C.; Jiang, G. H. Polymer vesicles with upper critical solution temperature for near-infrared light-triggered transdermal delivery of metformin in diabetic rats. *Chinese J. Polym. Sci.* **2022**, *40*, 157−165.
10 Yao, C. Z.; Wang, X. R.; Liu, G. H.; Hu, J. M.; Liu, S. Y. Distinct morphological transitions of photoreactive and thermoresponsive vesicles for controlled release and nanoreactors. *Macromolecules* **2016**, *49*, 8282−8295.
11 Lee, D.; Kim, J.; Ku, K. H.; Li, S.; Shin, J. J.; Kim, B. J. Poly(vinylpyridine)-containing block copolymers for smart, multicompartment particles. *Polym. Chem.* **2022**, *13*, 2570−2588.
12 Wu, Y. Q.; Wang, K.; Tan, H. Y.; Xu, J. P.; Zhu, J. T. Emulsion solvent evaporation-induced self-assembly of block copolymers containing pH-sensitive block. *Langmuir* **2017**, *33*, 9889−9896.
13 Ji, D.; Wang, Y. P.; Luo, M. Q.; Zhang, Z. H.; Chang, X. H.; Zhu, Y. T. pH and light-triggered shape transformation of block copolymer particles in emulsion droplets. *Eur. Polym. J.* **2024**, *221*, 113561.
14 Chen, M.; Li, J. W.; Zhang, W. J.; Hong, C. Y.; Pan, C. Y. pH-and reductant-responsive polymeric vesicles with robust membrane-cross-linked structures: In situ cross-linking in polymerization-induced self-assembly. *Macromolecules* **2019**, *52*, 1140-1149.
15 Lomas, H.; Canton, I.; MacNeil, S.; Du, J.; Armes, S. P.; Ryan, A. J.; Lewis, A. L.; Battaglia, G. Biomimetic pH sensitive polymersomes for efficient DNA encapsulation and delivery. *Adv. Mater.* **2007**, *19*, 4238−4243.
16 Japir, A.; Lu, N. N.; Wang, Y. H.; Mukerabigwi, J. F.; Zhou, Q. H.; Ge, Z. S. Membrane-cross-linked polymersomes with tumor ph-tunable selective permeability as intelligent nanoreactors and drug delivery vehicles. *Eur. Polym. J.* **2020**, *138*, 109982.
17 Li, J. J.; Li, Y. F.; Wang, Y. H.; Ke, W. D.; Chen, W. J.; Wang, W. P.; Ge, Z. S. Polymer prodrug-based nanoreactors activated by tumor acidity for orchestrated oxidation/chemotherapy. *Nano Lett.* **2017**, *17*, 6983−6990.
18 He, J.; Cao, J. P.; Chen, Y.; Zhang, L.; Tan, J. B. Thermoresponsive block copolymer vesicles by visible light-initiated seeded polymerization-induced self-assembly for temperature-regulated enzymatic nanoreactors. *ACS Macro Lett.* **2020**, *9*, 533−539.
19 Zhang, Y.; Uthaman, S.; Song, W.; Eom, K. H.; Jeon, S. H.; Huh, K. M.; Babu, A.; Park, I. K.; Kim, I. Multistimuli-responsive polymeric vesicles for accelerated drug release in chemo-photothermal therapy. *ACS Biomater. Sci. Eng.* **2020**, *6*, 5012−5023.
20 Nishimura, T.; Shishi, S.; Sasaki, Y.; Akiyoshi, K. Thermoresponsive polysaccharide graft polymer vesicles with tunable size and structural memory. *J. Am. Chem. Soc.* **2020**, *142*, 11784−11790.
21 Liu, F.; Kozlovskaya, V.; Medipelli, S.; Xue, B.; Ahmad, F.; Saeed, M.; Cropek, D.; Kharlampieva, E. Temperature-sensitive polymersomes for controlled delivery of anticancer drugs. *Chem. Mater.* **2015**, *27*, 7945−7956.
22 Halperin, A.; Kröger, M.; Winnik, F. M. Poly(N-isopropylacrylamide) phase diagrams: Fifty years of research. *Angew. Chem. Int. Ed.* **2015**, *54*, 15342−15367.
23 Beauté, L.; McClenaghan, N.; Lecommandoux, S. Photo-triggered polymer nanomedicines: From molecular mechanisms to therapeutic applications. *Adv. Drug Deliv. Rev.* **2019**, *138*, 148−166.
24 Wang, D. R.; Wang, X. G. Amphiphilic azo polymers: Molecular engineering, self-assembly and photoresponsive properties. *Prog. Polym. Sci.* **2013**, *38*, 271−301.
25 Ye, Q. Q.; Huo, M.; Zeng, M.; Liu, L.; Peng, L.; Wang, X. S.; Yuan, J. Y. Photoinduced reversible worm-to-vesicle transformation of azo-containing block copolymer assemblies prepared by polymerization-induced self-assembly. *Macromolecules* **2018**, *51*, 3308−3314.
26 Yu, X.; Li, J. L.; Zhang, J. N.; Jin, J.; Pan, Y. X.; Ji, X. L.; Jiang, W. Pathway-dependent shape transformation of polymeric vesicles under UV light and the assembly of UV-irradiated polymer. *Langmuir* **2024**, *40*, 17630−17637.
27 Wang, X. R.; Hu, J. M.; Liu, G. H.; Tian, J.; Wang, H. J.; Gong, M.; Liu, S. Y. Reversibly switching bilayer permeability and release modules of photochromic polymersomes stabilized by cooperative noncovalent interactions. *J. Am. Chem. Soc.* **2015**, *137*, 15262−15275.
28 Sun, Z. C.; Xu, Z. J.; Ding, M. Y.; Wang, L. Q.; Zhao, L.; Sui, P. L.; Li, G. D.; Jin, H. B.; Zhou, Y. F.; Lin, S. L. Ultrathin polymersomes with controllable light-responsivity via adjusting the electronic effect from *para*-substituents of azobenzene. *Angew. Chem. Int. Ed.* **2025**, *64*, e202503104.
29 Arai, N.; Yasuoka, K.; Zeng, X. C. Self-assembly of janus oligomers

into onion-like vesicles with layer-by-layer water discharging capability: A minimalist model. *ACS Nano* **2016**, *10*, 8026–8037.
30 Liu, D.; Zhang, Z. H.; Wang, R.; Hu, J. L. Stability and deformation of vesicles in a cylindrical flow. *Langmuir* **2022**, *38*, 629–637.
31 Wu, F. S.; Lin, J. P.; Wang, L. Q.; Lin, S. L. Polymer vesicles in a nanochannel under flow fields: a DPD simulation study. *Macromol. Theory Simul.* **2022**, *31*, 2200027.
32 Tseng, Y. C.; Chang, H. Y.; Sheng, Y. J.; Tsao, H. K. Atypical vesicles and membranes with monolayer and multilayer structures formed by graft copolymers with diblock side-chains: Nonlamellar structures and curvature-enhanced permeability. *Soft Matter* **2022**, *18*, 7559–7568.
33 Wang, T. Y.; Tsao, H. K.; Sheng, Y. J. Perforated vesicles of ABA triblock copolymers with on/off-switchable nanopores. *Macromolecules* **2020**, *53*, 10582–10590.
34 Jia, L.; Wang, R.; Fan, Y. N. Encapsulation and release of drug nanoparticles in functional polymeric vesicles. *Soft Matter* **2020**, *16*, 3088–3095.
35 Luo, Z. L.; Jiang, J. W. pH-sensitive drug loading/releasing in amphiphilic copolymer PAE-PEG: Integrating molecular dynamics and dissipative particle dynamics simulations. *J. Control. Release* **2012**, *162*, 185–193.
36 Luo, Z. L.; Li, Y.; Wang, B. B.; Jiang, J. W. pH-sensitive vesicles formed by amphiphilic grafted copolymers with tunable membrane permeability for drug loading/release: a multiscale simulation study. *Macromolecules* **2016**, *49*, 6084–6094.
37 Ma, S. Y.; Xiao, M. Y.; Wang, R. Formation and structural characteristics of thermosensitive multiblock copolymer vesicles. *Langmuir* **2013**, *29*, 16010–16017.
38 Feng, X.; Yan, N.; Jin, J.; Jiang, W. Disassembly of amphiphilic AB block copolymer vesicles in selective solvents: A molecular dynamics simulation study. *Macromolecules* **2023**, *56*, 2560–2567.
39 Zong, Y. Q.; Cui, J.; Han, Y. Y. Composition conversion-induced disassembly of amphiphilic ABA triblock copolymer vesicles: a Monte Carlo study. *Langmuir* **2025**, *41*, 3434–3443.
40 Zhao, R. X.; Zhou, W. T.; Zong, Y. Q.; Han, Y. Y.; Cui, J. Composition conversion-induced formation of multicompartment structures in the ordered aggregates of ABA triblock copolymers: a Monte Carlo study. *Acta Polymerica Sinica* (in Chinese) **2026**, *57*, 998–1010.
41 Zhou, W. T.; Zhao, R. X.; Zong, Y. Q.; Yan, C. X.; Han, Y. Y.; Cui, J. Monte Carlo simulation of chain architecture transition induced morphological transformation of diblock copolymer vesicle. *Polym. Bull.* (in Chinese) **2026**, *39*, 438–446.
42 Brannan, A. K.; Bates, F. S. ABCA tetrablock copolymer vesicles. *Macromolecules* **2004**, *37*, 8816–8819.
43 Stoenescu, R.; Graff, A.; Meier, W. Asymmetric ABC-triblock copolymer membranes induce a directed insertion of membrane proteins. *Macromol. Biosci.* **2004**, *4*, 930–935.
44 Carmesin, I.; Kremer, K. The bond fluctuation method: A new effective algorithm for the dynamics of polymers in all spatial dimensions. *Macromolecules* **1988**, *21*, 2819–2823.
45 Larson, R. Monte Carlo lattice simulation of amphiphilic systems in two and three dimensions. *J. Chem. Phys.* **1988**, *89*, 1642.
46 Larson, R. Monte Carlo simulation of microstructural transitions in surfactant systems. *J. Chem. Phys.* **1992**, *96*, 7904.
47 Hu, W. Structural transformation in the collapse transition of the single flexible homopolymer model. *J. Chem. Phys.* **1998**, *109*, 3686.
48 Haire, K.; Carver, T.; Windle, A. A Monte Carlo lattice model for chain diffusion in dense polymer systems and its interlocking with molecular dynamics simulation. *Comput. Theor. Polym. Sci.* **2001**, *11*, 17–28.
49 Ji, S.; Ding, J. Spontaneous formation of vesicles from mixed amphiphiles with dispersed molecular weight: Monte Carlo simulation. *Langmuir* **2006**, *22*, 553–559.
50 Metropolis, N.; Rosenbluth, A. W.; Rosenbluth, M. N.; Teller, A. H.; Teller, E. Equation of state calculations by fast computing machines. *J. Chem. Phys.* **1953**, *21*, 1087.
51 Cui, J.; Jiang, W. Structure of ABCA tetrablock copolymer vesicles and their formation in selective solvents: A Monte Carlo study. *Langmuir* **2011**, *27*, 10141–10147.
52 Ma, J. N.; Cui, J.; Han, Y. Y.; Jiang, W.; Sun, Y. C. Monte Carlo study of the micelles constructed by ABCA tetrablock copolymers and their formation in A-selective solvents. *RSC Adv.* **2015**, *5*, 86473–86484.
53 Uddin, M. A.; Yu, H. J.; Wang, L.; Ul Amin, B.; Mehmood, S.; Liang, R. X.; Haq, F.; Hu, J.; Xu, J. M. Dynamics in controllable stimuli-responsive self-assembly of polymer vesicles with stable radical functionality. *ACS Appl. Mater. Interfaces* **2021**, *13*, 61693–61706.
54 Tan, H. Y.; Liu, Y. Y.; Xie, J.; Gao, Y. J.; Li, Y. C.; Ma, L.; Zhang, L. B.; Tang, T.; Zhu, J. T. Light-triggered disassembly of photo-responsive gold nanovesicles for controlled drug release. *Mater. Chem. Front* **2020**, *4*, 2805–2811.
55 Tan, M.; Sun, F.; Zhao, X. Y.; Zhao, Z. B.; Zhang, S. R.; Xu, X. N.; Adijiang, A.; Zhang, W.; Wang, H. Y.; Wang, C. K.; Li, Z.; Scheer, E.; Xiang, D. Conductance evolution of photoisomeric single-molecule junctions under ultraviolet irradiation and mechanical stretching. *J. Am. Chem. Soc.* **2024**, *146*, 6856–6865.
56 Discher, D. E.; Eisenberg, A. Polymer vesicles. *Science* **2002**, *297*, 967–973.

https://doi.org/10.1007/s10118-026-3778-3